Available online at www.sciencedirect.com
SCIENCE DIRECT®
Chemical Physics 314 (2005) 37–47
Chemical Physics
www.elsevier.com/locate/chemphys

State-to-state reaction rates in gases with vibration–electronic–dissociation coupling: the influence on a radiative shock heated CO flow

A. Aliat [a,*], E.V. Kustova [b,*], A. Chikhaoui [c]

[a] ONERA-CERT/DMAE, 2 avenue Edouard Belin-BP 4025, Toulouse, France
[b] Department of Mathematics and Mechanics, Saint Petersburg State University, 28, Universitetski pr., Saint Petersburg 198504, Russia
[c] IUSTI – UMR 6595, Université de Provence, 13453 Marseille Cedex 13, France

Received 22 July 2004; accepted 14 January 2005
Available online 17 February 2005

Abstract

In the present paper, a theoretical model for the state specific dissociation–recombination rate coefficients taking into account electronically excited molecular states is proposed. The dissociation model generalizes the well known Treanor–Marrone model whereas the recombination model is derived using the microscopic detailed balance principle. The developed models are then applied for the investigation of a non-equilibrium high temperature CO flow with strongly coupled vibrational and electronic energy transitions, dissociation, recombination, and radiative transitions. The influence of dissociation from electronically excited states on the flow parameters is found to be important.

Keywords: State-to-state reaction rate coefficients; VT and VE transitions; Dissociation; Recombination; IR and UV radiation; Non-equilibrium gas flow; Shock wave; Carbon monoxide

1. Introduction

It is well known that in strongly non-equilibrium high temperature reacting gas flows, some of elementary physical–chemical processes like vibrational and electronic energy exchanges, and chemical reactions often proceed at the gas dynamic time scale, i.e. they go simultaneously with the change of macroscopic flow parameters. Such a coupling shown both experimentally and theoretically [1] provides a convincing argument against using multi-temperature and one-temperature non-equilibrium flow descriptions based on some quasi-stationary molecular distributions over internal energies. Moreover, accurate calculations of the rate coefficients of physical–chemical processes [2–6] confirm that the assumption about a strong difference between the characteristic times of vibrational transitions and chemical reactions, which provides a basis for quasi-stationary models, is violated under high temperature conditions.

Another point is that radiative processes are often considered independently from the collisional processes on the basis of the local thermal equilibrium (LTE) assumption. This uncoupled description can imply noticeable errors in estimated values of radiation intensities and radiative heat flux from strongly non-equilibrium flow regions.

These aspects of non-equilibrium kinetics have led to a rapid development of state-to-state models for the description of real gas flows with internal energy

* Corresponding authors. Tel.: +33 5 62 25 25 25; fax: +33 5 62 25 25 83 (A. Aliat), Tel.: +7 81 2428 4198; fax: +7 81 2428 6944 (E.V. Kustova).
E-mail addresses: Aziz.Aliat@polytech.univ-mrs.fr (A. Aliat), elena_kustova@mail.ru (E.V. Kustova).

0301-0104/$ - see front matter © 2005 Elsevier B.V. All rights reserved.
doi:10.1016/j.chemphys.2005.01.016

transitions, chemical reactions and radiation [1,7,8]. The state-to-state approach has the main advantage to treat directly vibrational level populations thus avoiding to introduce any quasi-stationary distributions over vibrational energy (the Boltzmann, Treanor ones or their modifications). In [8], a state-to-state model taking into account a strong coupling between the radiative and physical–chemical processes was developed. In [9,10], this model was extended to take into account molecular electronic states, i.e vibration–electronic (VE) energy transfers as well as the radiative transitions from the electronically excited states. In [10,11], the developed models were applied for the numerical investigation of a non-equilibrium reactive and radiative CO flow behind a shock wave. This allowed one to study the evolution of the vibrational level populations for each electronic state as well as the macroscopic flow parameters and radiation intensities behind a shock wave. However the model has been still limited by the assumption that molecules can dissociate only from the ground electronic state, which is not the case in high temperature flows.

Recently, a dissociation model taking into account electronically excited states was proposed in [12], and the effect of electronic excitation on the state-to-state dissociation rate coefficients was studied. However, an important question raises: has the model properly accounting for electronic excitation a real impact on the macroscopic flow field parameters or this effect can be neglected in numerical simulations? This issue still remains open. The objective of the present paper is to accomplish the study started in [12]. First, the theoretical model is completed by deriving expressions for the state specific recombination rate coefficients for each vibrational and electronic level. Then, developed models of dissociation and recombination are applied for the simulation of a shock heated CO flow. A substantial effect of dissociation–recombination involving electronically excited states on the vibrational distributions, gas flow parameters and radiation is found, which gives a good reason to recommend the new model for using in computational fluid dynamics.

2. Kinetic model

In [8–10], a non-equilibrium reactive and radiative gas flow is described on the basis of the kinetic equations for distribution functions in the spatial and temporal coordinates $(\mathbf{r},t)$. The atomic and molecular species are characterized by their chemical sort c, electronic α, vibrational i and rotational j states. The photons are specified by their frequency ν. A gas flow is considered under the following condition:

$$\tau_{\mathrm{el}} \sim \tau_{\mathrm{RR}} \sim \tau_{\mathrm{RT}} \ll \tau_{\mathrm{VV}} \sim \tau_{\mathrm{VT}} \sim \tau_{\mathrm{VE}} \sim \tau_{\mathrm{chem}} \sim \tau_{\mathrm{rad}} \sim \theta, \tag{1}$$

where τ_{el}, τ_{RR}, τ_{RT}, τ_{VV}, τ_{VT}, τ_{VE}, τ_{chem}, τ_{rad} indicate respectively the characteristic times of the elastic collisions, Rotation–Rotation (RR), Rotation–Translation (RT), Vibration–Vibration (VV), Vibration–Translation (VT), Vibration–Electronic (VE), chemical and radiative processes; θ is the mean time of macroscopic parameters change. It is proved experimentally [1,13] that condition (1) holds in a wide temperature range, in particular, it describes very well high enthalpy and high temperature hypersonic flows. This relation provides a basis for the state-to-state description of a non-equilibrium flow.

Distribution functions satisfy the Boltzmann equations modified to take into account internal degrees of freedom and chemical reactions as well as different rates of elementary processes. Asymptotic methods for solution of these kinetic equations are developed in [7,14] on the basis of the Chapman–Enskog method. The modification takes into account the fact that characteristic times of various elementary physical–chemical processes differ by several orders of magnitude, moreover, some of the microscopic processes proceed at the macroscopic time scale. The modified Chapman–Enskog method allows one to give a self-consistent description of a non-equilibrium flow appropriate to a specific relation between the characteristic relaxation times.

Under condition (1), using the modified Chapman–Enskog method [7,8,15], the zero order distribution functions of chemical species are found in the form:

$$f^{(0)}_{\mathrm{at},c} = \left(\frac{m_c}{2\pi kT}\right)^{3/2} n_{\mathrm{at},c} \exp\left(-\frac{m_c \mathbf{C}_c^2}{2kT}\right) \tag{2}$$

for atomic species, and

$$f^{(0)}_{c\alpha ij} = \left(\frac{m_c}{2\pi kT}\right)^{3/2} \frac{n_{c\alpha i} s_j^{c\alpha i}}{Z_{\mathrm{rot}}^{c\alpha i}} \exp\left(-\frac{m_c \mathbf{C}_c^2}{2kT} - \frac{\varepsilon_j^{c\alpha i}}{kT}\right) \tag{3}$$

for the populations of electro-vibrational levels of molecular species. Here, m_c and k are respectively the species c mass and the Boltzmann constant; $n_{\mathrm{at},c}$ is the number density of atoms c, $n_{c\alpha i}$ is the number density of molecules c at the electro-vibrational state (α,i); $\mathbf{C}_c = \mathbf{u}_c - \mathbf{v}$ is the peculiar velocity where $\mathbf{v}$ is the macroscopic gas velocity. Terms $s_j^{c\alpha i}, \varepsilon_j^{c\alpha i}$ and $Z_{\mathrm{rot}}^{c\alpha i}$ are respectively the rotational statistical weight, rotational energy of level j and the rotational partition function at the corresponding electro-vibrational state of a molecule.

Distribution functions (2) and (3) represent local equilibrium Maxwell distributions of molecules and atoms over velocities, and the Boltzmann distribution of molecules over rotational energy at the gas temperature T. Non-equilibrium atom number densities $n_{\mathrm{at},c}$ and electro-vibrational level populations $n_{c\alpha i}$ are found as solutions of master equations. One can notice that distribution functions (2) and (3) are expressed in terms

of macroscopic parameters $n_{\mathrm{at},c}(\mathbf{r},t)$, $n_{c\alpha i}(\mathbf{r},t)$, $\mathbf{v}(\mathbf{r},t)$ and $T(\mathbf{r},t)$.

Since the photon distribution function changes at the macroscopic time scale (see Eq. (1)), no macroscopic parameters can be assigned to the photon distributions in the frame of the Chapman–Enskog method. Therefore the distribution functions of photons are to be found directly from the microscopic kinetic equations which, introducing the specific radiation intensity I_ν, can be rewritten in the form of equations of radiative transfer [8,10].

Finally, macroscopic parameters $n_{\mathrm{at},c}(\mathbf{r},t)$, $n_{c\alpha i}(\mathbf{r},t)$, $\mathbf{v}(\mathbf{r},t)$, $T(\mathbf{r},t)$ together with the specific radiation intensity $I_\nu(\mathbf{r},t)$ form a reduced set of variables which provides a closed self consistent flow description in the state-to-state approach. A system of governing equations for these variables was derived in the general form in [8–10]. It includes the equations of vibration–electronic–chemical–radiative kinetics for the vibrational level populations, equations of chemical kinetics for atomic number densities, conservation of momentum and total energy, and equations of radiative transfer.

In the Euler approximation for a stationary one-dimensional gas flow behind a shock, the system of governing equations reads:

$$\frac{\mathrm{d}(vn_{\mathrm{at},c})}{\mathrm{d}x} = R_{\mathrm{at},c}, \tag{4}$$

$$\frac{\mathrm{d}(vn_{c\alpha i})}{\mathrm{d}x} = R_{c\alpha i}, \tag{5}$$

$$\rho v\frac{\mathrm{d}v}{\mathrm{d}x} + \frac{\mathrm{d}p}{\mathrm{d}x} = 0, \tag{6}$$

$$\rho v\frac{\mathrm{d}u}{\mathrm{d}x} + \frac{\mathrm{d}q_{\mathrm{rad}}}{\mathrm{d}x} + p\frac{\mathrm{d}v}{\mathrm{d}x} = 0, \tag{7}$$

$$\frac{\mathrm{d}I_\nu}{\mathrm{d}x} = R_\nu^{\mathrm{rad}}. \tag{8}$$

The variable x corresponds to the direction of the shock wave propagation, v is the flow velocity in the x direction; $p = nkT$ is the pressure (n is the total number density), ρ is the gas mixture density and u is the total energy of material particles per unit mass. It should be noted that the radiative flux q_{rad} appears in Eq. (7) due to the coupling of physical–chemical and radiative processes. This strong coupling is also introduced by the molecular production term in Eq. (5). Indeed, this term represents the sum of several terms responsible for various processes:

$$R_{c\alpha i} = R_{c\alpha i}^{\mathrm{VV}} + R_{c\alpha i}^{\mathrm{VT}} + R_{c\alpha i}^{\mathrm{VE}} + R_{c\alpha i}^{\mathrm{chem}} + R_{c\alpha i}^{\mathrm{rad}}. \tag{9}$$

The term $R_{c\alpha i}^{\mathrm{rad}}$ is associated to radiative processes and can be written as [11]:

$$\begin{aligned} R_{c\alpha i}^{\mathrm{rad}} = {} & 4\pi\sum_{\alpha'<\alpha}\sum_{i'}\int_0^\infty \mathrm{d}\nu\Phi^c_{\nu,\alpha i\alpha' i'} \\ & \times\left[-n_{c\alpha i}A^c_{\alpha i\alpha' i'} + \left(n_{c\alpha' i'}B^c_{\alpha' i'\alpha i} - n_{c\alpha i}B^c_{\alpha i\alpha' i'}\right)I_\nu\right] \\ & - 4\pi\sum_{\alpha''>\alpha}\sum_{i''}\int_0^\infty \mathrm{d}\nu\Phi^c_{\nu,\alpha'' i''\alpha i}\left[-n_{c\alpha'' i''}A^c_{\alpha'' i''\alpha i}\right. \\ & \left. + \left(n_{c\alpha i}B^c_{\alpha i\alpha'' i''} - n_{c\alpha'' i''}B^c_{\alpha'' i''\alpha i}\right)I_\nu\right]. \end{aligned} \tag{10}$$

These radiative source terms have been derived taking into account the isotropic character of the radiation field, the existence of the Boltzmann distribution over rotational energy and the normalizing conditions for the Hönl–London factors [10]. The band profile function $\Phi^c_{\nu,\alpha i\alpha' i'}$ associated to the transition $(\alpha i \to \alpha' i')$ satisfies the normalizing condition [16]:

$$\int_0^\infty \mathrm{d}\nu\Phi^c_{\nu,\alpha i\alpha' i'} = 1. \tag{11}$$

The terms $A^c_{\alpha i\alpha' i'}$, $B^c_{\alpha i\alpha' i'}$ and $B^c_{\alpha' i'\alpha i}$ in Eq. (10) correspond to the band Einstein coefficients for absorption, induced and spontaneous emission, respectively. In the present study, they are calculated using the data for CO molecules given in [17–19]. The expression for the radiative production term in Eq. (8) depends on the spectral Einstein coefficients and can be found in [10,11].

Let us discuss now the production terms in Eq. (5) due to the vibrational energy exchanges. In [10,11] it is shown that the vibration–vibration (VV) transitions do not affect the evolution of vibrational distributions and macroscopic parameters in a high temperature reacting CO flow behind the shock. Since we consider a similar flow in the present study, the VV processes are neglected hereafter.

The production term in Eq. (9) associated to the VT vibrational energy exchanges reads:

$$R_{c\alpha i}^{\mathrm{VT}} = \sum_M n_M\sum_{i'\neq i}\left(k^M_{c\alpha,i'i}n_{c\alpha i'} - k^M_{c\alpha,ii'}n_{c\alpha i}\right), \tag{12}$$

where M indicates a collision partner with the number density n_M. Coefficients $k^M_{c\alpha,ii'}(i \to i')$ and $k^M_{c\alpha,i'i}(i' \to i)$ in the production term (12) are the rate coefficients of the VT process described by the following reaction:

$$A_{c\alpha i} + M \rightleftharpoons A_{c\alpha i'} + M. \tag{13}$$

Modelling of the state specific rate coefficients for vibrational energy exchanges is widely discussed in the literature. Exact quantum calculations [2–4] provide a good accuracy but appear to be rather computationally laborious. They are often used for the validation of more approximate approaches [20–22]. Approximate analytic expressions for the rate coefficients are also in common use in kinetic modelling, mainly because of their simplicity. One of the most popular models is the Schwartz, Slawsky, Herzfeld one [23] based on the first-order perturbation theory; its generalization for anharmonic oscillators is given in [24,25]. It works rather well for low quantum vibrational states but fails

at high collision velocities, high quantum numbers and can not be applied for multi-quantum processes ($|i' - i| > 1$ in reaction (13)). A more rigorous theoretical approach is used in the nonperturbative forced harmonic oscillator (FHO) model elaborated in [26–29]. The FHO model takes into account the coupling of many vibrational states during a collision and is therefore, applicable for high temperature conditions and multi-quantum jumps.

Unfortunately, the direct use of accurate trajectory methods and complete FHO model in computational fluid dynamics codes is hardly possible due to their complexity, and therefore some time saving approximations are required for numerical simulations. For this purpose, interpolations of experimental measurements or quantum calculations can be used. Comparing three-dimensional semi-classical calculations by Cacciatore and Billing [30] and experimental data [31,32] on the VV and VT transition probabilities in CO with the results obtained by means of analytical models, we can recommend the asymptotic model proposed by Nikitin and Osipov [33] for the calculation of the FHO transitions probabilities [10,11]. This asymptotic model saves noticeably the computational time especially for the energy exchange at high vibrational quantum numbers. We also utilize expressions given by Adamovich and Rich [34] to calculate the steric factor to take into account the effects of realistic three-dimensional collisions and molecular rotation. In the present study, the steric factor for the VT monoquantum transitions is supposed to be equal $1/\pi$ which corresponds to the expected theoretical value 1/3 [29].

The production term in (9) due to the VE exchange has the form

$$R^{\mathrm{VE}}_{c\alpha i} = \sum_M n_M \sum_{\alpha' \neq \alpha} \sum_{i'} \left(k^M_{c\alpha' i' \alpha i} n_{c\alpha' i'} - k^M_{c\alpha i \alpha' i'} n_{c\alpha i} \right), \tag{14}$$

where $k^M_{c\alpha i \alpha' i'}(\alpha i \to \alpha' i')$ and $k^M_{c\alpha' i' \alpha i}(\alpha' i' \to \alpha i)$ are the rate coefficients of the VE energy transitions described by the following reaction

$$A_{c\alpha i} + M \rightleftharpoons A_{c\alpha' i'} + M. \tag{15}$$

The VE transitions are very effective when the electro-vibrational levels (α,i) and (α',i') are isoenergetic. The data for the rate coefficients of these processes for CO molecules can be found in [32].

Let us turn to the production terms by chemical reactions. In this study, only one reaction of dissociation and recombination is considered

$$A_{c\alpha i} + M \rightleftharpoons A_f + A_g + M. \tag{16}$$

Atoms f and g are the components of the diatomic molecule c. Atomic species are assumed to be in the ground electronic state. Then the chemical production terms in Eqs. (4) and (5) read:

$$R_{\mathrm{at},c} = R^{\mathrm{diss\text{–}rec}}_{\mathrm{at},c}, \quad R^{\mathrm{chem}}_{c\alpha i} = R^{\mathrm{diss\text{–}rec}}_{c\alpha i}, \tag{17}$$

with

$$R^{\mathrm{diss\text{–}rec}}_{\mathrm{at},c} = -\sum_{\alpha i} R^{\mathrm{diss\text{–}rec}}_{c\alpha i}. \tag{18}$$

The molecular dissociation–recombination production term has the form

$$R^{\mathrm{diss\text{–}rec}}_{c\alpha i} = \sum_M n_M \left(k^{\mathrm{rec},M}_{c\alpha i} n_{\mathrm{at},f} n_{\mathrm{at},g} - k^{\mathrm{diss},M}_{c\alpha i} n_{c\alpha i} \right), \tag{19}$$

where $k^{\mathrm{diss},M}_{c\alpha i}$ and $k^{\mathrm{rec},M}_{c\alpha i}$ are respectively the state-to-state dissociation and recombination rate coefficients.

Modelling of the dissociation–recombination rate coefficients is one of the crucial points for the correct prediction of vibrational distributions and gas dynamic parameters. The most reliable data on the reactive cross sections are obtained by means of quantum and quasi-classical dynamical approaches. We can refer to works [35–45] by Clary, Miller, Laganà, Gilibert with coauthors which present accurate data for specific reactions in molecular systems containing H_2, D_2, OH, H_2O, N_2, O_2, NO and other species including electronically excited states. Unfortunately, the number of reactions studied using quantum and semiclassical methods is rather limited. Moreover, a direct use of these precise but extremely time consuming methods in computational fluid dynamics is possible only by exploiting computing grid technologies [46–48] which at present time are still under development. That is why in numerical simulations, simpler but less accurate models are commonly used. There exist a variety of phenomenological and few analytical dissociation models, one can find an exhaustive list of models in [49], among them the ladder-climbing model, Treanor–Marrone [50], Macheret [51] models and other ones. These models are based on different physical assumptions and thus have various degree of accuracy. However, the common issue is that they describe dissociation only from the ground electronic state, which is not satisfactory in high temperature and high enthalpy flows.

Recently, a generalization of the Treanor–Marrone model, which accounts for electronic excitation has been proposed in [12]. In this paper, the state-to-state rate coefficient of species c dissociation from the ith vibrational level of the electronic state α $k^{\mathrm{diss},M}_{c\alpha i}$ is expressed in terms of the thermal equilibrium rate coefficient $k^{\mathrm{diss},M}_{c,\mathrm{eq}}$ and a non-equilibrium factor $\mathscr{Z}_{c\alpha i}$

$$k^{\mathrm{diss},M}_{c\alpha i} = \mathscr{Z}_{c\alpha i} k^{\mathrm{diss},M}_{c,\mathrm{eq}}. \tag{20}$$

The thermal equilibrium coefficients can be found using the Arrhenius law whereas the following expression for the generalized non-equilibrium factor $\mathscr{Z}_{c\alpha i}$ is obtained in [12]:

$$\mathscr{Z}_{c\alpha i}(T,U) = Z^c_{\mathrm{el}}(T) \exp\left(\frac{\varepsilon^{c\alpha}_i + \varepsilon^c_\alpha}{k} \left[\frac{1}{T} + \frac{1}{U} \right] \right) \times \left[\sum_\beta s^c_\beta \exp\left(\frac{\varepsilon^c_\beta}{kU} \right) \frac{Z^{c\beta}_{\mathrm{vibr}}(-U)}{Z^{c\beta}_{\mathrm{vibr}}(T)} \right]^{-1}, \tag{21}$$

where $Z^c_{\rm el}, s^c_\alpha$ are the partition function and statistical weight of the electronic state α:

$$Z^c_{\rm el}(T) = \sum_\alpha s^c_\alpha \exp\left(-\varepsilon^c_\alpha/kT\right), \tag{22}$$

$Z^{c\alpha}_{\rm vibr}$ is the vibrational partition function for the given electronic state:

$$Z^{c\alpha}_{\rm vibr}(T) = \sum_i \exp\left(-\varepsilon^{c\alpha}_i/kT\right), \tag{23}$$

(the vibrational statistical weight $s^{c\alpha}_i$ is equal to unit for diatomic molecules); $\varepsilon^{c\alpha}_i, \varepsilon^c_\alpha$ are the vibrational and electronic energy of corresponding states; T is the gas temperature; U is an adjustable parameter which has a dimension of a temperature and describes how rapidly the dissociation probability decreases for low levels. It is shown in [52] that in the general case, parameter U should depend on the temperature and on the vibrational state of the molecule especially at low temperatures and high vibrational levels. However, in the whole range of temperature and quantum vibrational states setting U equal to a fraction of the molecular dissociation energy $\vartheta_{\rm diss}$ leads to a satisfactory agreement.

The factor $\mathscr{Z}_{c\alpha i}$ represents a state-to-state vibration–electronic–dissociation coupling factor for preferential dissociation from highly excited electronic and vibrational levels. If only the ground electronic state of a molecule c is taken into account, expression (21) reduces to a state dependent vibration–dissociation coupling factor obtained by several authors (for instance, in [52]):

$$\mathscr{Z}_{ci}(T,U) = \frac{Z^c_{\rm vibr}(T)}{Z^c_{\rm vibr}(-U)} \exp\left(\frac{\varepsilon^c_i}{k}\left[\frac{1}{T}+\frac{1}{U}\right]\right). \tag{24}$$

The value of parameter $U=\infty$ corresponds to the case of non-preferential dissociation from any vibrational level.

Fig. 1 presents the temperature dependence of the state-to-state rate coefficient $k^{\rm diss,CO}_{{\rm CO},\alpha,1}$ for CO dissociation

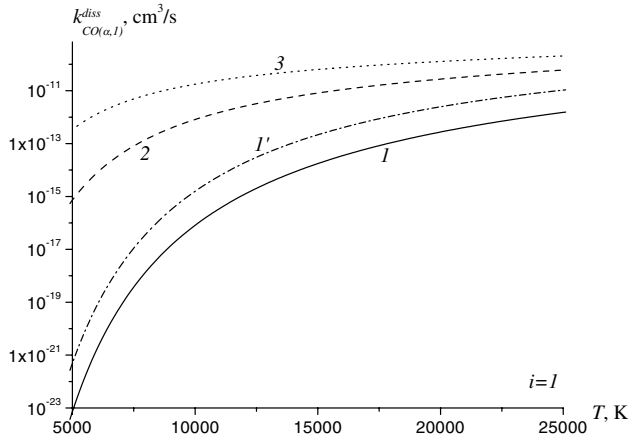

Fig. 1. Rate coefficients $k^{\rm diss}_{{\rm CO},\alpha,1}$ of dissociation from different electronic levels. Curves *1, 2, 3* correspond to the electronic states $X^1\Sigma$, $a^3\Pi$, $A^1\Pi$. *1′* corresponds to $k^{\rm diss}_{{\rm CO},X^1\Sigma,1}$ calculated using formula (24).

from the first vibrational level of various electronic states in the temperature range 5000–25,000 K for the case of preferential dissociation ($U=3T$). The coefficient of dissociation from the ground electronic state is calculated using both expressions (21) and (24). One can see that all rate coefficients increase with temperature, the rate of dissociation from excited electronic states exceeds noticeably the corresponding rate for lower states. Taking into account several excited electronic levels leads to a considerably lower rate of dissociation from the ground electronic state; it is explained by the repartition of internal energy between electronic states [12].

Let us derive now the state-to-state rate coefficients of recombination. They can be obtained by means of kinetic theory methods using the principle of microscopic reversibility. Indeed, the chemical production term (19) is connected to the microscopic integral operator of the dissociation–recombination reaction $J^{\rm diss-rec}_{c\alpha ij}$ by the formula:

$$R^{\rm diss-rec}_{c\alpha i} = \sum_j \int {\rm d}\mathbf{u}_c\, J^{\rm diss-rec}_{c\alpha ij}, \tag{25}$$

where

$$J^{\rm diss}_{c\alpha ij} = \sum_M \int {\rm d}\mathbf{u}_f {\rm d}\mathbf{u}_g {\rm d}\mathbf{u}'_M {\rm d}\mathbf{u}_M {\rm d}\mathbf{u}_c \times \left[\frac{f_f}{m_f^3}\frac{f_g}{m_g^3}\frac{f_M(\mathbf{u}'_M)}{m_M^3} W^{c\alpha ij,M}_{f,g,M} - \frac{f_{c\alpha ij}}{m_c^3}\frac{f_M(\mathbf{u}_M)}{m_M^3}\ W^{f,g,M}_{c\alpha ij,M}\right]. \tag{26}$$

In the last expression, $W^{f,g,M}_{c\alpha ij,M}$ is the probability per unit time of the reaction between a particle of c species with the velocity $\mathbf{u}_c$ and internal states (α, i, j) and a particle M with the velocity $\mathbf{u}_M$ leading to the formation of species $(f,\ g,\ M)$ with the velocities $(\mathbf{u}_f, \mathbf{u}_g, \mathbf{u}'_M)$. The prime indicates the change of the particle M velocity during the reaction. The term $W^{c\alpha ij,M}_{f,g,M}$ corresponds to the probability per unit time of the backward reaction, i.e. recombination. It is essentially assumed that the particle M is structureless or it does not change its internal state during the reaction.

Substituting the distribution functions (2) and (3) to expression (26), using conservation of the total energy in a dissociation–recombination reaction:

$$\frac{m_c C_c^2}{2} + \varepsilon^c_\alpha + \varepsilon^{c\alpha}_i + \varepsilon^{c\alpha i}_j + \varepsilon^c_f + \frac{m_M C_M^2}{2} = \frac{m_f C_f^2}{2} + \varepsilon^f_f + \frac{m_g C_g^2}{2} + \varepsilon^g_f + \frac{m_M C_M'^2}{2} \tag{27}$$

(ε^c_f is the formation energy of the species c), and finally applying the principle of microscopic reversibility [14,53,54]:

$${\rm d}\mathbf{u}_M {\rm d}\mathbf{u}_c W^{f,g,M}_{c\alpha ij,M} h^3 s^c_\alpha s^{c\alpha}_i s^{c\alpha i}_j = {\rm d}\mathbf{u}_f {\rm d}\mathbf{u}_g {\rm d}\mathbf{u}'_M W^{c\alpha ij,M}_{f,g,M} \tag{28}$$

(h is the Planck constant, $s_i^{c\alpha} = 1$ for diatomic species), the production term (25) can be reduced to the form (19) with the state-to-state recombination rate coefficient connected to that of dissociation by the relation:

$$k_{c\alpha i}^{\mathrm{rec},M} = k_{c\alpha i}^{\mathrm{diss},M} \left(\frac{m_c}{m_f m_g}\right)^{3/2} s_\alpha^c (2\pi kT)^{-3/2} h^3 Z_{\mathrm{rot}}^{c\alpha i}(T) \exp\left(-\frac{\Delta\varepsilon}{kT}\right). \tag{29}$$

Here, $\Delta\varepsilon$ is the energy variation during the collision:

$$\Delta\varepsilon = \varepsilon_\alpha^c + \varepsilon_i^{c\alpha} + \varepsilon_f^c - \varepsilon_f^f - \varepsilon_f^g. \tag{30}$$

It should be noted that Eq. (29) generalizes the well known expression connecting the dissociation and recombination rate coefficients for the ground electronic state [7]. Indeed, taking into account only fundamental electronic state, one can easily obtain the following relation:

$$k_{ci}^{\mathrm{rec},M} = k_{ci}^{\mathrm{diss},M} \left(\frac{m_c}{m_f m_g}\right)^{3/2} (2\pi kT)^{-3/2} h^3 Z_{\mathrm{rot}}^{ci}(T) \exp\left(-\frac{\Delta\varepsilon}{kT}\right), \tag{31}$$

with the variation of energy

$$\Delta\varepsilon = \varepsilon_i^{c\alpha} + \varepsilon_f^c - \varepsilon_f^f - \varepsilon_f^g. \tag{32}$$

This last relation is identical to the one given in [7].

Let us note that the ratio

$$K_{c\alpha i} = \frac{k_{ci}^{\mathrm{rec},M}}{k_{c\alpha i}^{\mathrm{rec},M}} \tag{33}$$

of the recombination rate coefficients (29) and (31) depends on the ratio of the corresponding state-to-state dissociation rate coefficients and thus can be expressed in terms of the ratio of vibration–dissociation and vibration–electronic–dissociation coupling factors $\mathscr{Z}_{\mathrm{ci}}$ and $\mathscr{Z}_{c\alpha i}$. For the ground electronic state, it does not depend on the vibrational level: $K_{c\alpha i} = K_{c\alpha}$ (for instance, when $\alpha = X^1\Sigma$ for CO molecules).

Fig. 2 presents the temperature dependence of the recombination rate coefficients for the CO ground electronic state $X^1\Sigma$ and vibrational levels $i = 1$, 15, 30. The values of $k_{\mathrm{CO},X^1\Sigma,i}^{\mathrm{rec,CO}}$ are obtained using both formula (29) taking into account the first three electronic energy levels ($X^1\Sigma$,$a^3\Pi$,$A^1\Pi$) and formula (31) for only the ground electronic state. The rate coefficients are calculated for $U = \vartheta_{\mathrm{diss}}/6$ (preferential dissociation) and $U = \infty$ (non-preferential dissociation).

One can notice that taking into account excited electronic states leads to a reduction of the recombination rate coefficients. This decrease is stronger in the case of the preferential dissociation model when the ratio (33) can reach approximately a factor 30 (see Fig. 3). This ratio is about 5 in the non-preferential case, and varies weakly with the temperature. Let us emphasize that if only the fundamental electronic state is taken into account, for upper vibrational levels, the recombination rate coefficient for the preferential case becomes higher than that for the non-preferential model. It is not the case when three electronic states are taken into account.

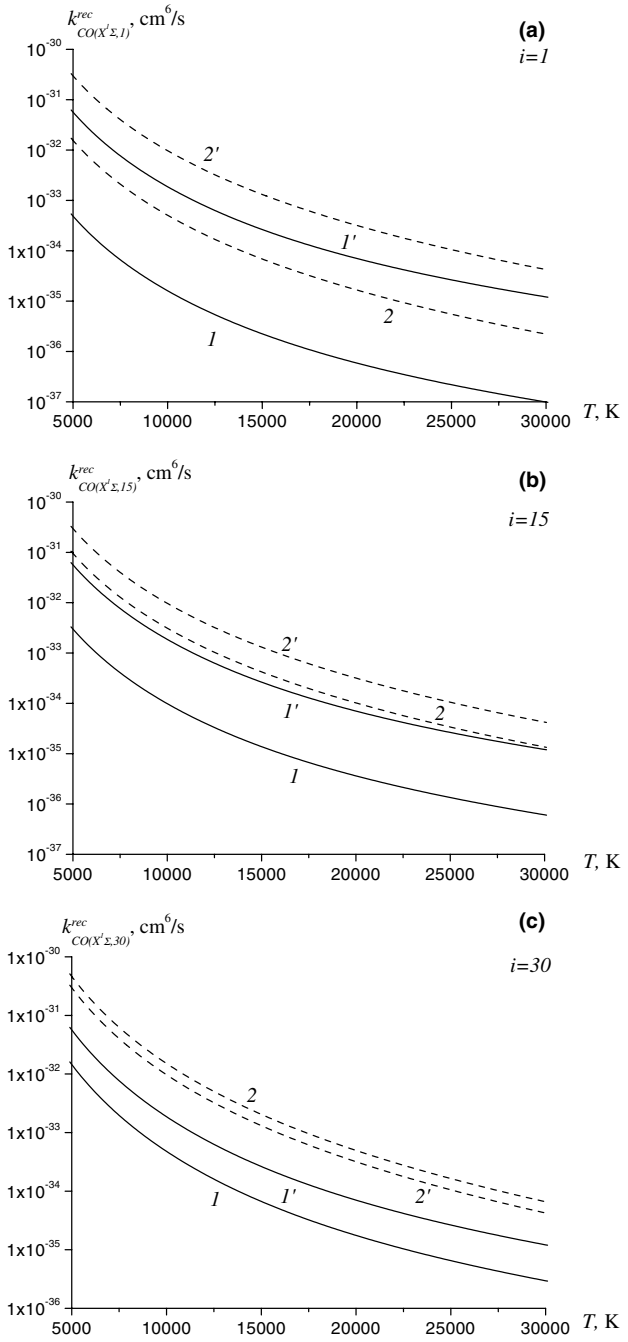

Fig. 2. Rate coefficient $k_{\mathrm{CO},X^1\Sigma,i}^{\mathrm{rec}}$ of recombination as a function of temperature. (a) $i = 1$; (b) $i = 15$; (c) $i = 30$. Curves *1, 1′* are obtained using formula (29); *2′, 2′* with formula (31). *1, 2* for $U = \vartheta_{\mathrm{diss}}/6$; *1′, 2′* for $U = \infty$.

Fig. 4 shows that recombination of CO molecules is more effective for high vibrational states. Fig. 5 illustrates the temperature dependence of the recombination rate coefficients of CO molecules at the

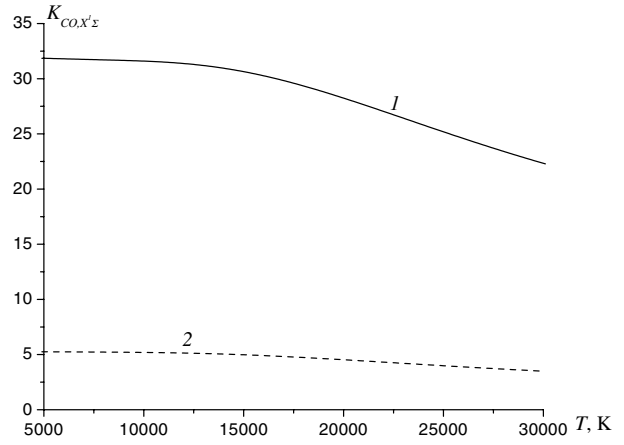

Fig. 3. Ratio $K_{\mathrm{CO}(X^1\Sigma)}$ of the recombination rate coefficients as a function of temperature. *1*: $U = \vartheta_{\mathrm{diss}}/6$; *2*: $U = \infty$.

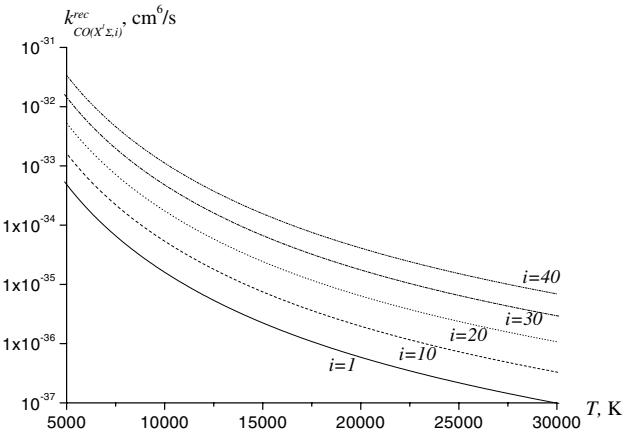

Fig. 4. Recombination rate coefficients $k^{\mathrm{rec}}_{\mathrm{CO}(X^1\Sigma,i)}$ $(i = 1, 10, 20, 30, 40)$ as functions of temperature. $U = \vartheta_{\mathrm{diss}}/6$.

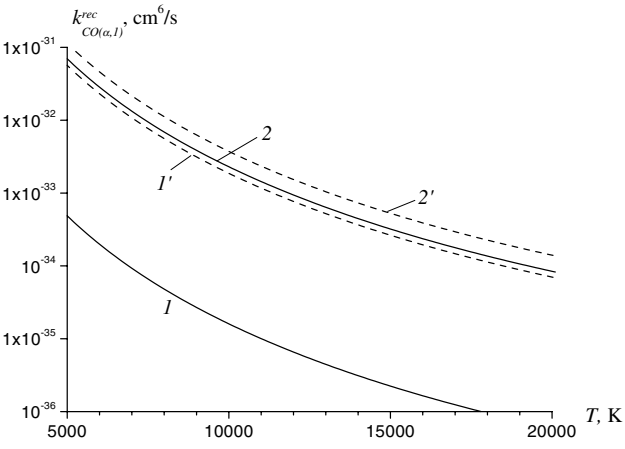

Fig. 5. Recombination rate coefficients $k^{\mathrm{rec}}_{\mathrm{CO}(\alpha,1)}$ as functions of temperature. *1*, *1′* correspond to the electronic states $X^1\Sigma$; *2*, *2′* to $A^1\Pi$; *1*, *2*: $U = \vartheta_{\mathrm{diss}}/6$; *1′*, *2′*: $U = \infty$.

electronic states $X^1\Sigma$ and $A^1\Pi$, and vibrational level $i = 1$. One can see that recombination to the excited electronic state is more effective, the ratio of the recombination rate coefficients associated to the electronic states $A^1\Pi$ and $X^1\Sigma$ can reach 100. It is interesting to note, that for the ground electronic state, the preferential character of dissociation changes considerably the rate coefficients whereas for the $A^1\Pi$ state, the rate coefficients for preferential and non-preferential models are close to each other.

In the thermochemical equilibrium, the populations of the electronic and vibrational levels follow the Boltzmann distributions with the gas temperature T. Therefore, the relation between the molecular and atomic number densities takes the form [10]

$$\frac{n_{\mathrm{at},g}n_{\mathrm{at},f}}{n_c} = \left(\frac{m_f m_g}{m_c}\right)^{3/2}(2\pi kT)^{3/2}h^{-3}[Z^c_{\mathrm{el}}(T)Z^c_{\mathrm{vib}}(T)Z^c_{\mathrm{rot}}(T)]^{-1} \times \exp\left(\frac{\varepsilon^c_f - \varepsilon^f_f - \varepsilon^g_f}{kT}\right), \tag{34}$$

which expresses the mass action law in gases with electronic excitation.

3. Applications

In this section, a steady-state one-dimensional inviscid CO flow behind a plane shock wave is studied. It is assumed that the mixture is constituted of CO molecules at the ground electronic state $X^1\Sigma$ and excited electronic states $a^3\Pi$ and $A^1\Pi$, and atoms C and O in their fundamental state ^3P. The elementary processes taking place in the flow are the VT transitions:

$$\mathrm{CO}(\alpha, i) + M \rightleftharpoons \mathrm{CO}(\alpha, i') + M, \tag{35}$$

the near-resonant VE exchanges:

$$\mathrm{CO}(X^1\Sigma, i \sim 27) + M \rightleftharpoons \mathrm{CO}(a^3\Pi, i \sim 0) + M, \tag{36}$$

$$\mathrm{CO}(X^1\Sigma, i \sim 40) + M \rightleftharpoons \mathrm{CO}(A^1\Pi, i \sim 0) + M, \tag{37}$$

which are known to be important in optically pumped systems [18,55,56].

We also take into account dissociation and recombination of CO molecules at their fundamental and excited electronic states:

$$\begin{aligned} &\mathrm{CO}(X^1\Sigma, i) + M \rightleftharpoons \mathrm{C}(^3P) + \mathrm{O}(^3P) + M,\\ &\mathrm{CO}(a^3\Pi, i) + M \rightleftharpoons \mathrm{C}(^3P) + \mathrm{O}(^3P) + M,\\ &\mathrm{CO}(A^1\Pi, i) + M \rightleftharpoons \mathrm{C}(^3P) + \mathrm{O}(^3P) + M. \end{aligned} \tag{38}$$

The state specific rate coefficients of these reactions are developed in the previous section. The thermal equilibrium rate coefficient for CO dissociation are computed using the data from [57].

Two range of radiative transitions are considered: IR radiation due to the transitions between vibrational levels of the fundamental electronic state, and UV and visible radiation caused by the transitions between electronic states. The most intense bands observed in the UV and visible range are the CO fourth positive band due to the transitions between electronics states $A^1\Pi$ and $X^1\Sigma$. Among radiative transitions the induced emission and absorption

$$\mathrm{CO}(\alpha, i) + hv \rightleftharpoons \mathrm{CO}(\alpha', i') + 2hv, \tag{39}$$

and spontaneous emission

$$\mathrm{CO}(\alpha, i) \rightarrow \mathrm{CO}(\alpha', i') + hv \tag{40}$$

are distinguished.

4. Results and discussions

A gas upstream the shock is initially composed of pure CO at the ambient temperature 300 K, with a pressure of 500 Pa. The speed of the shock wave is 5200 m/s. We study here the influence of electronic states on the evolution of vibrational distributions and various macroscopic variables in a flow behind the shock. The preferential dissociation model with $U = 3T$ is chosen.

First, let us analyze the influence of VE and radiative transitions on vibrational distributions and macroscopic parameters. The contribution of VE processes (36) and (37) to the formation of vibrational distributions in a shock heated CO is found to be very weak compared to the role of these transitions in low temperature CO systems [31], where a strong depletion of the ground electronic state vibrational levels close to $i = 26$ and $i = 40$ has been observed. In the high temperature case, the rate of dissociation from the upper vibrational states appears to be much higher than the rate of VE transitions [11], and thermal decomposition of CO molecules becomes dominant compared to VE transitions from the ground electronic state. However VE transitions provide a source of electronically excited molecules and thus influence significantly the dissociation process and the UV emission intensity.

Concerning the role of radiative transitions, our calculation show that while the distributions over vibrational and electronic energy are the main factors determining the IR and UV radiation intensity, the inverse effect of radiation on the distributions and macroscopic parameters is practically negligible. An exception is the population of electronically excited states which depends strongly on the radiative transitions.

Further discussion is focused on the impact of dissociation and recombination involving electronically excited states on gas dynamic parameters, vibrational distributions and radiation. In order to study this effect, we have applied two models of the dissociation–recombination rate coefficients described in Section 2: taking into account three CO electronic states (model *1*) and only the ground state (model *2*). The results are given below.

Fig. 6 presents the time evolution of atomic molar fractions behind the shock wave for the case of preferential dissociation ($U = 3T$). One can see that dissociation from only the ground electronic state $X^1\Sigma$ provides a faster atomic production behind the shock. It is not unexpected: analyzing the dissociation rate coefficients (see Fig. 1) one can conclude that the rate of dissociation from the ground electronic state is considerably higher (curves *1* and *1′*), therefore neglecting higher electronic states in the dissociation model leads to a noticeable overestimation of the atomic production rate.

From the theoretical point of view, model *1* seems to be much more accurate compared to the model *2*. Nevertheless, practical recommendations on the choice of the model can be done only after its validation in terms of experimental results. Unfortunately, no experimental data on the gas dynamic parameters distribution behind a shock wave for a chosen molecular system are available in the literature. We have found only one criterion for the model validation: experimentally measured dissociation incubation time [58]. The bold vertical line in Fig. 6 represents the CO dissociation incubation time τ_{inc} measured by Appleton in a shock tube at $T \approx 13{,}000$ K which corresponds to our test case conditions just after the shock front ($T = 12{,}920$ K). One can see that the model *1* provides a satisfactory agreement with the experiment (at $t = \tau_{\mathrm{inc}}$ the molar fraction of atoms is less than 1%) whereas the model *2* taking into account only ground electronic state dissociation, gives the calculated incubation time shorter than the measured one by an order of magnitude. Thus, we conclude that the model *1* accounting for dissociation from ex-

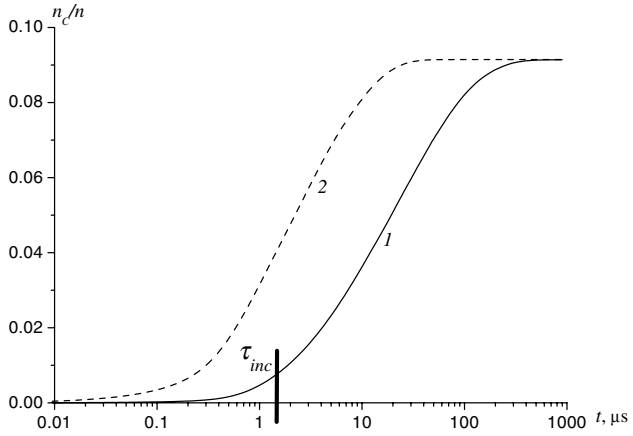

Fig. 6. Atomic molar fraction as a function of time. *1*: dissociation from $X^1\Sigma$, $a^3\Pi$, $A^1\Pi$ states; *2*: dissociation from $X^1\Sigma$ state. Bold vertical line corresponds to the experimentally measured incubation time of dissociation [58].

cited electronic states is more suitable for the description of a high temperature flow behind a shock wave.

Fig. 7 presents the evolution of translational–rotational temperature T with the distance x behind the shock front. The temperature relaxation is considerably faster in the case when only ground electronic state takes part in dissociation. For this model, thermal equilibrium is attained at $x \approx 3$–5 cm whereas for the model *1*, the relaxation zone becomes approximately ten times longer. Nonetheless, the equilibrium temperature value attained at the end of the relaxation zone, coincides for both models *1* and *2*. The high rate of thermal equilibration found using the model *2* can be explained by the fact that fast dissociation removes more energy from the translational mode and thus decreases rapidly temperature values.

This conclusion is confirmed by Fig. 8 which illustrates the vibrational distribution of CO($X^1\Sigma$) molecules. In this figure the mass fractions $\rho_{CO,X^1\Sigma,i}/\rho = m_{CO}n_{CO,X^1\Sigma,i}/\rho$ are plotted as functions of i. One can notice that molecules being at the intermediate and higher vibrational levels dissociate more quickly when only the ground electronic state takes part in dissociation. While the shape of vibrational distributions for the model *1* is close to the Boltzmann one, for the model *2*, fast dissociation process disturbs noticeably the tail of distribution.

Fig. 9 gives the mass fraction of the $A^1\Pi$ electronic state as a function of x. Neglecting dissociation from electronically excited states yields a lower population of the level $A^1\Pi$, a discrepancy may reach a factor 100 just behind the shock front. It is not surprising because in this case, dissociation of the highly excited vibrational levels of the ground electronic state proceeds faster compared to the case of dissociation from all electronic levels (see Fig. 8). Since levels $i \sim 40$ of the $X^1\Sigma$ state participating in the VE transition (37) are more depleted by the dissociation process, this VE transition becomes less efficient, and the concentration of the $A^1\Pi$ level occurs lower in the case of dissociation from only the ground electronic state.

As far as molecules CO($A^1\Pi$) are responsible for the UV emission, its intensity is found to be lower when neglecting dissociation from the excited electronic levels, especially close to the shock front (see Fig. 10). On the other hand, the IR radiation remains practically identical in both cases, because it is emitted essentially by the first vibrational levels of the $X^1\Sigma$ electronic state which are not affected by the dissociation model.

Finally, we can conclude that using the model *2* leads to a considerable loss of accuracy; it overestimates the dissociation rate and the rate of temperature relaxation, distorts the vibrational distributions, underestimates the electronic excitation rate and thus the intensity of UV radiation. When the electronic states are taken into account in dissociation, the total thermochemical

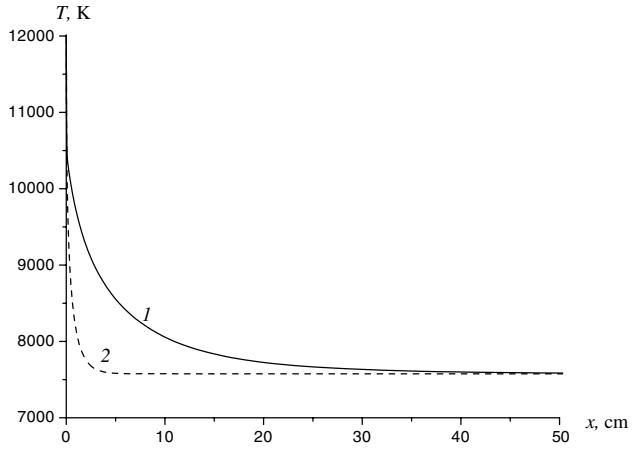

Fig. 7. Translational temperature as a function of the distance x behind the shock. *1*: dissociation from $X^1\Sigma$, $a^3\Pi$, $A^1\Pi$ states; *2*: dissociation from $X^1\Sigma$ state.

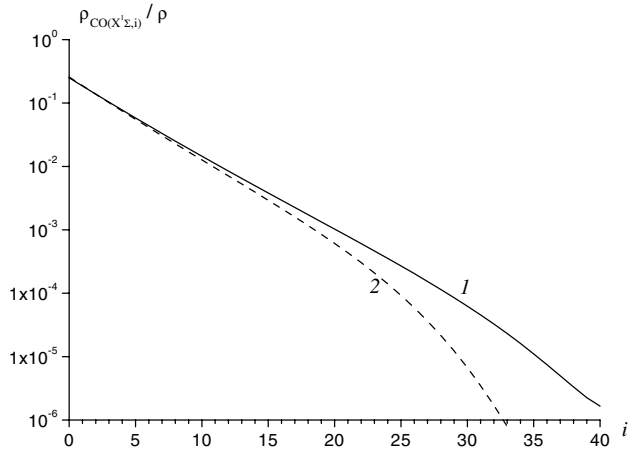

Fig. 8. Vibrational distribution of CO($X^1\Sigma$) molecules at $x = 0.1$ cm. *1*: dissociation from $X^1\Sigma$, $a^3\Pi$, $A^1\Pi$ states; *2*: dissociation from $X^1\Sigma$ state.

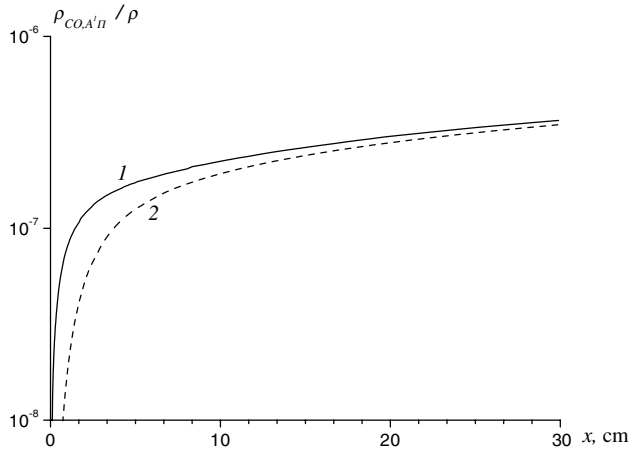

Fig. 9. Excited electronic state $A^1\Pi$ mass fraction as a function of x. *1*: dissociation from $X^1\Sigma$, $a^3\Pi$, $A^1\Pi$ states; *2*: dissociation from $X^1\Sigma$ state.

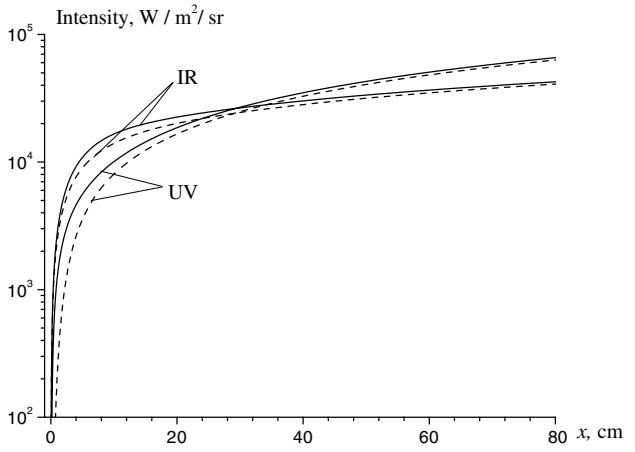

Fig. 10. IR and UV intensities as functions of x. Solid lines: dissociation from $X^1\Sigma$, $a^3\Pi$, $A^1\Pi$ states; dashed lines: dissociation from $X^1\Sigma$ state.

equilibrium is attained at a longer distance behind the shock: the length of the relaxation zone is about 30–40 cm in this case compared to 5 cm in the case of dissociation from only the $X^1\Sigma$ state. It can be seen from Fig. 11, where the ratio $\rho_C\rho_O/\rho_{CO}$ is plotted as a function of x. For a comparison, the same ratio calculated using expression (34) at a given temperature is presented. This last expression represents the ratio of the reaction products and reagents concentrations under chemically equilibrium conditions. One can notice a considerable deviation from the mass action law in the region of non-equilibrium chemical reactions.

The last figure, Fig. 12, illustrates the influence of the model parameter U on the gas temperature. This parameter determines the preferential character of dissociation. Two values of the parameter have been tested $U = 3T$, $U = \vartheta_{diss}/6k$ (ϑ_{diss} is the CO dissociation energy). It is seen that under the conditions of this study, the various values of U provide quasi-identical tempera-

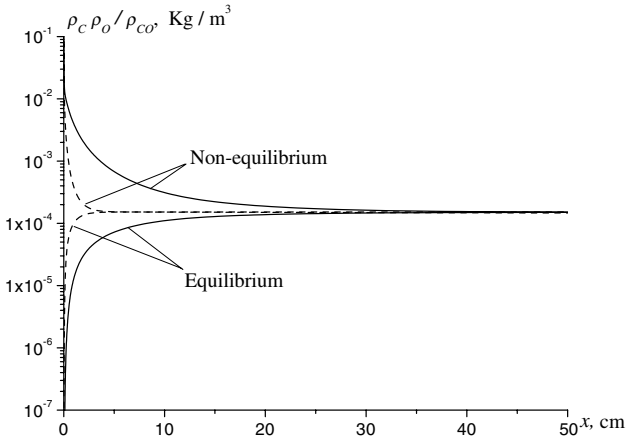

Fig. 11. Ratio $\rho_C\rho_O/\rho_{CO}$ as a function of x. Solid lines: dissociation from $X^1\Sigma$, $a^3\Pi$, $A^1\Pi$ states; dashed lines: dissociation from $X^1\Sigma$ state. Equilibrium ratio is calculated using formula (34); non-equilibrium ratio represents real flow conditions.

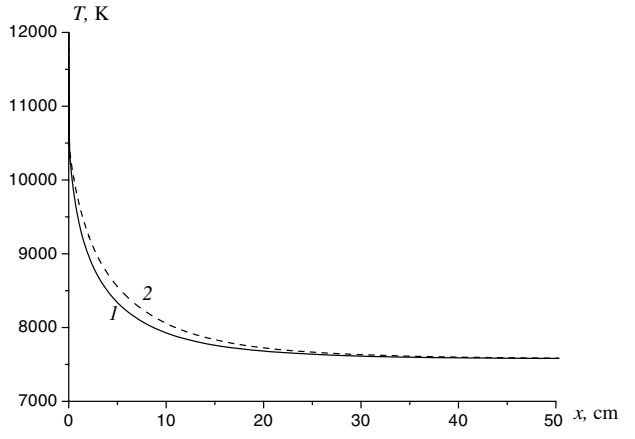

Fig. 12. Translational temperature as a function of x. *1*: $U = 3T$; *2*: $U = \vartheta_{diss}/6$.

ture relaxation. Similar results are obtained for the vibrational distributions and other flow parameters. It leads us to the conclusion that in dissociation modelling, the role of the parameter U appears to be much weaker compared to the effect of excited electronic states.

5. Conclusion

A theoretical model for the state specific dissociation–recombination rate coefficients for diatomic electronically excited molecules is proposed. Taking into account electronic states provides a decrease in the dissociation and recombination rate coefficients, the discrepancy is weak for the non-preferential dissociation model and increases for the preferential case. The reaction rate coefficients are greater for excited vibrational and electronic states.

The model developed in the paper needs further validation using rigorous quantum calculations and experimental results on the dissociation and recombination cross sections in electronically excited gases (which are still not available in the literature). However it can be used for the estimation of the role of the excited electronic states in high temperature kinetics.

Thus, it is shown that dissociation from the excited electronic states affects significantly the evolution of macroscopic variables in a non-equilibrium reactive and radiative CO gas flow behind a shock wave. Neglecting electronic states leads to significant errors in predicted values of high temperature non-equilibrium flow parameters, particularly, to an underestimation of the relaxation zone length.

Acknowledgement

This work has been supported by the French Space Agency CNES in the frame of the Mars Sample Return

Program. The study has been partially supported by INTAS (Grant No. 03-51-5204).

References

[1] M. Capitelli, C. Ferreira, B. Gordiets, A. Osipov, Plasma kinetics in atmospheric gasesSpringer Series on Atomic, Optical and Plasma Physics, vol. 31, Springer-Verlag, Berlin, 2000.
[2] G. Billing, E. Fisher, Chem. Phys. 43 (1979) 395.
[3] G. Billing, R. Kolesnick, Chem. Phys. Lett. 200 (4) (1992) 382.
[4] G. Billing, in: M. Capitelli (Ed.), Nonequilibrium Vibrational Kinetics, Springer-Verlag, Berlin, 1986, pp. 85–111.
[5] F. Esposito, M. Capitelli, Chem. Phys. Lett. 302 (1999) 49.
[6] F. Esposito, M. Capitelli, C. Gorse, Chem. Phys. 257 (2000) 193.
[7] E. Nagnibeda, E. Kustova, Kinetic Theory of Transport and Relaxation Processes in Nonequilibrium Reacting Gas Flows, Saint Petersburg University Press, Saint Petersburg, 2003.
[8] E. Kustova, A. Chikhaoui, Chem. Phys. 255 (2000) 59.
[9] E. Kustova, A. Aliat, A. Chikhaoui, Chem. Phys. Lett. 344 (5–6) (2001) 638.
[10] A. Aliat, Modélisation d'un écoulement hypersonique de CO en déséquilibre physico-chimique et radiatif derrière une onde de choc, Ph.D. thesis, Universitéde Provence, Marseille (2002).
[11] A. Aliat, A. Chikhaoui, E. Kustova, Phys. Rev. E 68 (2003) 056306.
[12] A. Aliat, E. Kustova, A. Chikhaoui, Chem. Phys. Lett. 390 (4–6) (2004) 37.
[13] Y. Stupochenko, S. Losev, A. Osipov, Relaxation in Shock Waves, Springer-Verlag, Berlin, Heidelberg, New York, 1967.
[14] S. Vallander, E. Nagnibeda, M. Rydalevskaya, Some Questions of the Kinetic Theory of the Chemical Reacting Gas Mixture, Leningrad University Press, Leningrad, 1977 (in Russian). Translation: US AirForce FASTC–ID (RS) TO–0608–93.
[15] A. Chikhaoui, J. Dudon, E. Kustova, E. Nagnibeda, Physica A 247 (1–4) (1997) 526.
[16] S. Gilles, W. Vincenti, J. Quant. Spectrosc. Radiat. Transfer 10 (1970) 71.
[17] H. Heaps, G. Herzberg, Z. Physik 133 (1953) 49.
[18] C. Flament, T. George, K. Meister, J. Tufts, J. Rich, V. Subramanian, J.-P. Martin, B. Piar, M.-Y. Perrin, Chem. Phys. 163 (1992) 241.
[19] B. Piar, Production de molécules excitées vibrationnellement et électroniquement par pompage laser. Analyse des états formés, Ph.D. thesis, Ecole Centrale Paris, Paris (1993).
[20] D. Secrest, B. Johnson, J. Chem. Phys. 45 (1966) 4556.
[21] X. Chapuisat, G. Bergeron, J.-M. Launay, Chem. Phys. 20 (1977) 285.
[22] X. Chapuisat, G. Bergeron, J.-M. Launay, Chem. Phys. 36 (1979) 397.
[23] R. Schwartz, Z. Slawsky, K. Herzfeld, J. Chem. Phys. 20 (1952) 1591.
[24] B. Gordiets, A. Osipov, L. Shelepin, Kinetic Processes in Gases and Molecular Lasers, Gordon and Breach Science Publishers, Amsterdam, 1988.
[25] R. Bray, J. Phys. B. (Proc. Phys. Soc.) 1 (2) (1968) 705.
[26] E. Kerner, Can. J. Phys. 36 (1958) 371.
[27] C. Treanor, J. Chem. Phys. 43 (1965) 532.
[28] A. Zelechow, D. Rapp, T. Sharp, J. Chem. Phys. 49 (1968) 286.
[29] I. Adamovich, S. Macheret, J. Rich, C. Treanor, AIAA J. 33 (6) (1995) 1064.
[30] M. Cacciatore, G. Billing, Chem. Phys. 58 (3) (1981) 395.
[31] R. Deleon, J. Rich, Chem. Phys. 107 (1986) 283.
[32] A. Chiroux de Gavelle de Roany, C. Flament, J. Rich, V. Subramaniam, W. Warren Jr., AIAA J. 31 (1) (1993) 119.
[33] E. Nikitin, A. Osipov, Vibrational relaxation in gasesKinetics and Catalysis, vol. 4, VINITI, All-Union Institute of Scientific and Technical Information, Moscow, 1977 (in Russian), chapter 2.
[34] I. Adamovich, J. Rich, AIAA Paper 99-3565.
[35] A. Wickham, D. Clary, J. Chem. Phys. 98 (1993) 420.
[36] D. Clary, AIP Conf. Proc. 312 (1994) 405.
[37] S. Pogrebnya, J. Echave, D. Clary, J. Chem. Phys. 107 (1997) 8975.
[38] D. Charlo, D. Clary, J. Chem. Phys. 117 (2002) 1660.
[39] B. Kerkeni, D. Clary, J. Chem. Phys. 121 (2004) 6809.
[40] V. Mandelshtam, H. Taylor, W. Miller, J. Chem. Phys. 105 (1996) 496.
[41] A. Viel, C. Leforestier, W. Miller, J. Chem. Phys. 108 (1998) 3489.
[42] T. Yamamoto, W. Miller, J. Chem. Phys. 118 (2003) 2135.
[43] W. Miller, Y. Zhao, M. Ceotto, S. Yang, J. Chem. Phys. 119 (2003) 1329.
[44] A. Laganà, E. Garcia, J. Chem. Phys. 98 (1994) 502.
[45] M. Gilibert, X. Gimenez, M. Gonzales, R. Sayos, A. Aguilar, Chem. Phys. 191 (1995) 1.
[46] O. Gervasi, A. Laganà, M. Lobbiani, Lecture Notes in Computer Science 2331 (2002) 956.
[47] O. Gervasi, A. Laganà, F. Sportolari, J. Comp. Meth. Science Eng. 2 (2002) 377.
[48] L. Storchi, C. Manuali, O. Gervasi, G. Vitillaro, A. Laganà, F. Tarantelli, Lecture Notes in Computer Science 2658 (2003) 297.
[49] Physical and Chemical Processes in Gas Dynamics: Cross Sections and Rate Constants for Physical and Chemical Processes. volume I, Vol. I96 of Progress in Astronautics and Aeronautics, 2002.
[50] P. Marrone, C. Treanor, Phys. Fluids 6 (9) (1963) 1215.
[51] S. Macheret, I. Adamovich, J. Chem. Phys. 113 (17) (2000) 7351.
[52] F. Esposito, M. Capitelli, E. Kustova, E. Nagnibeda, Chem. Phys. Lett. 330 (2000) 207.
[53] I. Kuščer, Phys. A 176 (1991) 542.
[54] B. Alexeev, A. Chikhaoui, I. Grushin, Phys. Rev. E 49 (1994) 2809.
[55] H. Wallaart, B. Piar, M.-Y. Perrin, J.-P. Martin, Chem. Phys. 196 (1995) 149.
[56] E. Plönjes, P. Palm, A. Chernukho, I. Adamovich, J. Rich, Chem. Phys. 256 (2000) 315.
[57] R. Hanson, J. Chem. Phys. 60 (12) (1974) 4970.
[58] J. Appleton, M. Steinberg, D. Liquornik, J. Chem. Phys. 52 (5) (1970) 2205.